



ELSEVIER

Journal of Crystal Growth 189/190 (1998) 172–177

JOURNAL OF **CRYSTAL  
GROWTH**

# Growth of single crystal GaN on a Si substrate using oxidized AlAs as an intermediate layer

Nobuhiko P. Kobayashi<sup>a,\*</sup>, Junko T. Kobayashi<sup>a</sup>, Won-Jin Choi<sup>b</sup>, P. Daniel Dapkus<sup>a,b</sup>,  
Xingang Zhang<sup>c</sup>, Daniel H. Rich<sup>c</sup>

<sup>a</sup> *Compound Semiconductor Laboratory, Department of Materials Science and Engineering, University of Southern California, Vivian Hall of Engineering, Los Angeles, California 90089-0241, USA*

<sup>b</sup> *Compound Semiconductor Laboratory, Department of Electrical Engineering – Electrophysics, University of Southern California, Power Hall of Engineering, Los Angeles, California 90089-0483, USA*

<sup>c</sup> *Photonic Materials and Devices Laboratory, Department of Materials Science and Engineering, University of Southern California, Vivian Hall of Engineering, Los Angeles, California 90089-0241, USA*

---

## Abstract

We demonstrate that single-crystal hexagonal GaN can be grown by metal-organic chemical vapor deposition on an aluminum oxide compound ( $\text{AlO}_x$ ) layer utilized as an intermediate layer between GaN and a Si(1 1 1) substrate. The surface morphology of GaN grown on the  $\text{AlO}_x/\text{Si}(1\ 1\ 1)$  substrate is found to be very sensitive to both the GaN buffer-layer thickness and the  $\text{AlO}_x$  thickness. Contact mode atomic force microscopy (C-AFM) observation indicates that the  $\text{AlO}_x$  surface is composed of domain-like features with varying surface heights. A possible clue for a mechanism by which single crystal GaN grows on  $\text{AlO}_x$  is discussed by comparing the domain-like surface features observed by C-AFM. © 1998 Elsevier Science B.V. All rights reserved.

*PACS:* 81.15.Gh; 81.10.Bk; 81.05.Ea; 78.60.Hk; 81.65.Mq; 68.35.Bs

*Keywords:* GaN; Aluminum oxide; MOCVD; CL; AFM; XRD

---

Sapphire has been the substrate most commonly used for growing III-nitrides and related alloys. Relatively, few attempts have been made to utilize Si as the substrate for III-nitride growth and, in most of these cases, an intermediate buffer layer

such as AlN [1], SiC [2] or nitridized GaAs [3] was used. In addition to these buffer layer approaches, the concept of a compliant substrate using a carbonized silicon-on-insulator substrate has also been proposed and experimentally explored [4,5]. In this paper, we propose and demonstrate the use of an oxidized aluminum arsenide ( $\text{AlO}_x$ ) layer as an intermediate layer to grow single-crystal GaN on a Si substrate. We are

---

\* Corresponding author. Tel.: + 1 213 740 6018; fax: + 1 213 740 8684; e-mail: nkobayas@scf.usc.edu.

motivated in this work to utilize the properties of the  $\text{AlO}_x$  to realize a compliant substrate when used in conjunction with the underlying Si substrate.

The samples studied were prepared in the following way (also see Fig. 1). An AlAs layer and a GaAs cap layer (300 Å) were grown (Fig. 1a) by atmospheric metal-organic chemical vapor deposition (MOCVD) on a chemically cleaned Si(1 1 1) substrate. Various AlAs-layer thicknesses were studied. A specular GaAs/AlAs surface was routinely obtained by employing a two-step growth procedure. Subsequently, the AlAs/GaAs layers were patterned and etched to expose the edges of the AlAs layer which was selectively oxidized and converted to  $\text{AlO}_x$  by heating in a water vapor/ $\text{N}_2$  ambient at 425°C for 1 h, then the GaAs cap layer was removed (Fig. 1b). A high temperature ( $\sim 1000^\circ\text{C}$ ) annealing was subsequently performed in  $\text{O}_2$ . Finally GaN was grown (Fig. 1c) on the  $\text{AlO}_x/\text{Si}(1\ 1\ 1)$  substrate (referred as  $\text{AlO}_x/\text{Si}(1\ 1\ 1)$

in this paper) by MOCVD using a multistep growth approach [6].

As previously reported [7], single crystal X-ray diffraction measurements ( $\theta$ - $2\theta$  mode) indicates that hexagonal single-crystal GaN is grown on  $\text{AlO}_x/\text{Si}(1\ 1\ 1)$  under the specific growth conditions used here, while GaN grown directly on Si(1 1 1) results in polycrystal phase. It is also found that  $\text{AlO}_x$  contains an amorphous/fine-grain phase [8].

Fig. 2a is a plan-view SEM image taken from GaN/ $\text{AlO}_x/\text{Si}(1\ 1\ 1)$ , showing an almost specular surface with several hexagonal pits. In the cross-sectional scanning electron microscope image shown in Fig. 2b, the  $\text{AlO}_x$  intermediate layer can be seen clearly between the GaN layer and the Si substrate. In Fig. 2c it is evident that GaN is predominantly grown on the area covered by the  $\text{AlO}_x$  layer.

Fig. 3 presents the cathodoluminescence (CL) spectrum taken from GaN grown on  $\text{AlO}_x/\text{Si}(1\ 1\ 1)$ . In addition to the emissions commonly seen, an additional broad-emission feature is seen, appearing to contain at least three different emission peaks near 3.155 eV. The origin of the broad emission is unknown. We speculate that it may be related to a deep level created by oxygen penetrating from  $\text{AlO}_x$  layer [9] but further investigation will be needed for positive identification.

The surface morphology is found to be very sensitive to the low-temperature GaN buffer-layer thickness ( $d_{\text{buffer}}$ ) grown on the  $\text{AlO}_x$  layer. The ratio of the smooth area to the total area, obtained

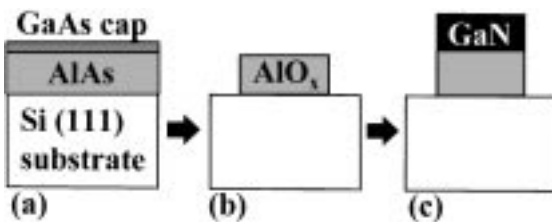


Fig. 1. Sample preparation procedure.

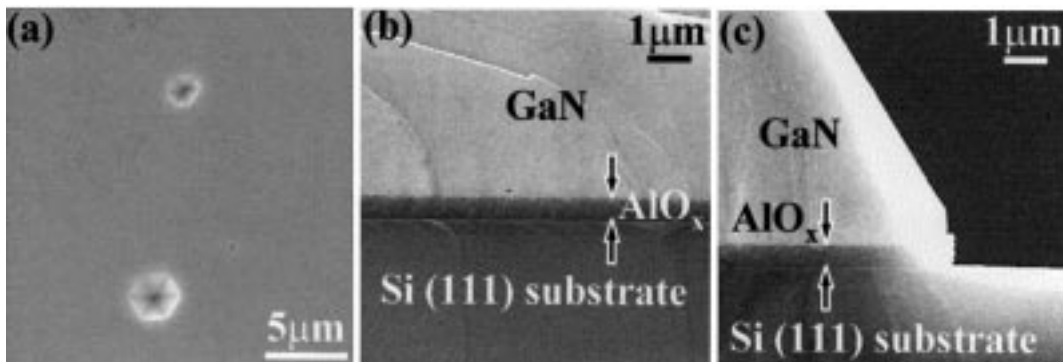


Fig. 2. SEM images of GaN grown on  $\text{AlO}_x/\text{Si}(1\ 1\ 1)$ .

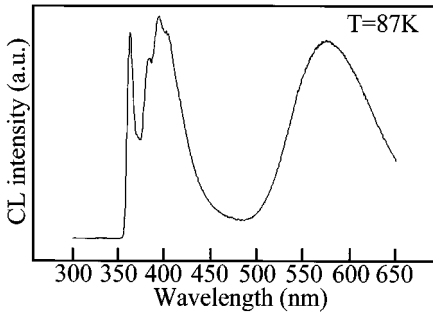


Fig. 3. Cathodoluminescence spectrum of GaN/AIO<sub>x</sub>/Si(1 1 1).

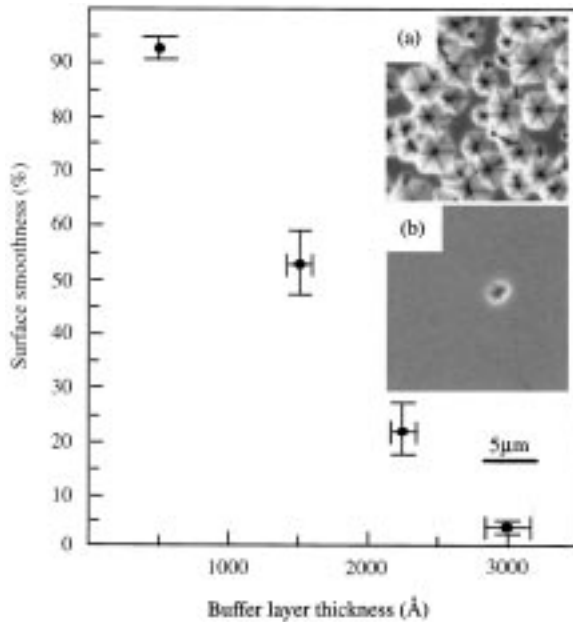


Fig. 4. Surface smoothness plotted as a function of  $d_{\text{buffer}}$ . The nominal thickness of GaN overlayer is  $\sim 4 \mu\text{m}$  for 3 h growth.  $d_{\text{AlOx}} = 2500 \text{ \AA}$  is fixed ( $d_{\text{buffer}}$  is variable).

by plan-view SEM, i.e. surface smoothness, is plotted as a function of  $d_{\text{buffer}}$  in Fig. 4. The ratio increases rapidly as  $d_{\text{buffer}}$  decreases. However, if no buffer layer is grown, randomly oriented crystallites appear on the surface. The trend seen in Fig. 4 indicate the optimum  $d_{\text{buffer}}$  in terms of the surface morphology will be in the range from 0 to 500 Å (The insets are plan-view SEM images of GaN grown for 3 hours with  $d_{\text{buffer}}$  is (a) 2250 Å and (b) 500 Å.)

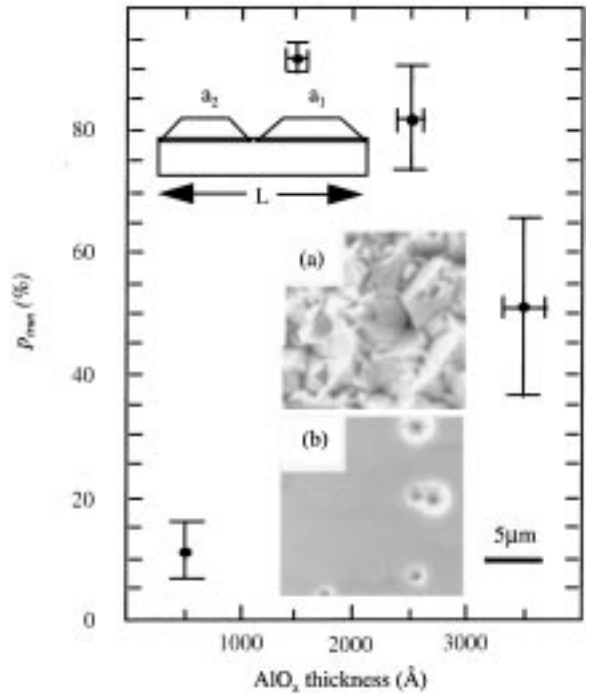


Fig. 5.  $P_{\text{trun}}$  is the sum of the segments ( $a_1, a_2, \dots$ ) that composes the flat surface divided by the total length ( $L$ ) measured in cross-sectional SEM images. The nominal thickness of GaN overlayer is  $\sim 4 \mu\text{m}$  for 3 h growth.  $d_{\text{buffer}} = 500 \text{ \AA}$  ( $d_{\text{AlOx}}$  is variable) is fixed.

The surface morphology is also found to be strongly influenced by the AlO<sub>x</sub> layer thickness ( $d_{\text{AlOx}}$ ) as shown in Fig. 5 in which  $P_{\text{trun}}$ , a measure of surface smoothness ( $P_{\text{trun}}$  approaches 100% as a surface becomes smoother), is defined in the figure caption.  $P_{\text{trun}}$  increases as  $d_{\text{AlOx}}$  decreases from 3500 Å, peaking at around  $d_{\text{AlOx}} = 1500 \text{ \AA}$ , then drops rapidly (The insets are plan-view SEM images of GaN grown for 3 h with  $d_{\text{AlOx}}$  is (a) 500 Å and (b) 1500 Å).

In Fig. 6 a similar tendency that shows a peak at around  $d_{\text{AlOx}} \sim 2000 \text{ \AA}$  is observed in the plot of the  $\omega$ -scan FWHM as a function of  $d_{\text{AlOx}}$  (Normalized CL I<sub>2</sub> line intensity is also plotted). The minimum FWHM obtained by a double-crystal X-ray diffraction  $\omega$ -scan is  $\sim 980 \text{ arcsec}$ . Although this value is comparable to the numbers reported for GaN grown directly on Si(1 1 1) [1,4], the factors contributing to our FWHM obtained on the

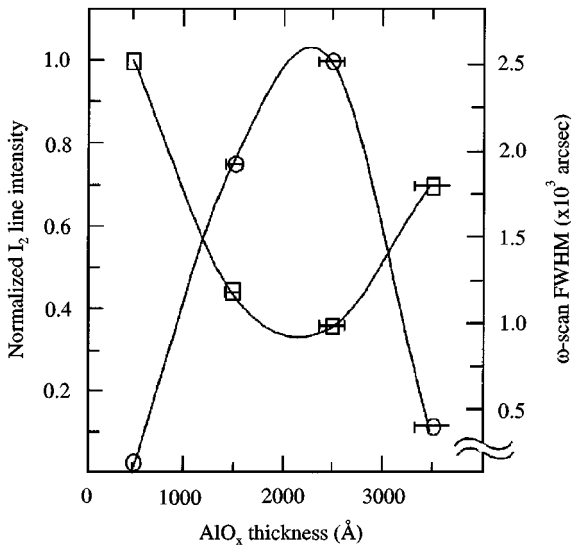


Fig. 6. Normalized I<sub>2</sub> line intensity and ω-scan FWHM as a function of AlO<sub>x</sub> thickness (open square: normalized I<sub>2</sub> line intensity, open circle: ω-scan FWHM)

line-and-space patterned GaN/AlO<sub>x</sub>/Si, resulted from the oxidation process, must be more complicated. The use of the patterned GaN/AlO<sub>x</sub> structure may have resulted in slight variations in the orientation of GaN grown on one pattern to another, which would cause an increased FWHM value.

Generally, in highly mismatched heteroepitaxy the macroscopic surface morphology and the ω-scan FWHM of an epitaxial layer are strongly influenced by the degree of the structural defects in the film. Thus, we believe that the similar tendency observed in Figs. 5 and 6 is most likely to be tied predominantly to the degree of structural defects in the GaN, which is expected to vary with  $d_{\text{AlO}_x}$ . Furthermore, inhomogeneous misfit strain accumulated in GaN, which is also expected to vary with  $d_{\text{AlO}_x}$ , may have partially contributed to the trend seen in Figs. 5 and 6.

We also examined the AlO<sub>x</sub> surface by C-AFM. Fig. 7 shows the AlO<sub>x</sub> surface topography taken at the different stages of the sample preparation prior to the GaN buffer-layer growth. The as-formed AlO<sub>x</sub> surface appears to consist of sparsely packed domain-like features (lateral scale of ~ 3500 Å)

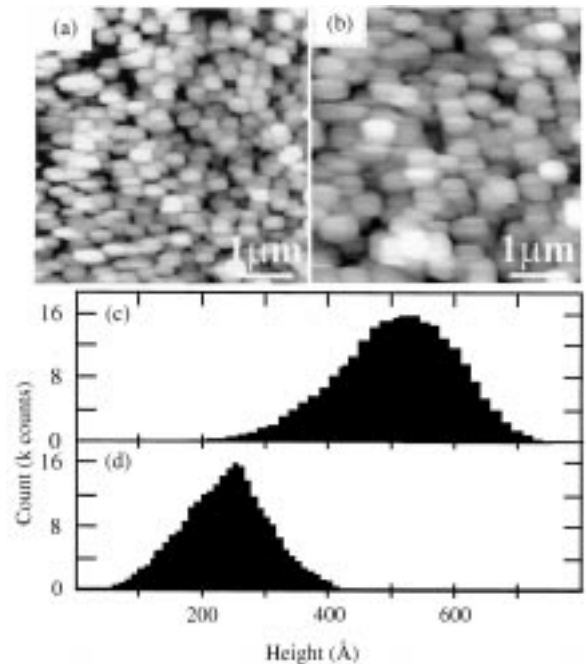


Fig. 7. AFM images taken from (a) as-grown AlO<sub>x</sub> layer and (b) AlO<sub>x</sub> layer after a high-temperature annealing followed by a post growth annealing. The high-temperature annealing was performed at 1000°C in O<sub>2</sub> for 1 h and the post growth annealing was done at 1000°C in H<sub>2</sub> for 1 h.

that have a distribution of heights resulting in an r.m.s. roughness of 102 Å (see the corresponding histogram in (c)). As shown in (b), the lateral size of the domain-like feature increases (~ 7000 Å) upon annealing, resulting in a smoother surface (r.m.s. roughness of 56 Å) along with a reduction of the difference in heights as can be seen in the height histogram shown in (d). Since the surface of the AlO<sub>x</sub> layer consists of the domain-like features and a larger r.m.s. roughness compared to a typical sapphire substrate surface [10], we expect that the observed domain-like features have an impact on the nucleation and evolution of the subsequent GaN growth.

In Fig. 8, C-AFM images taken from the surface of the GaN buffer-layer (100 Å thick grown at 450°C) grown on sapphire (0 0 0 1) and AlO<sub>x</sub>/Si (1 1 1) are represented. The lateral size of domain-like features seen on the buffer-layer grown on AlO<sub>x</sub>/Si (1 1 1) is much larger than that on sapphire.

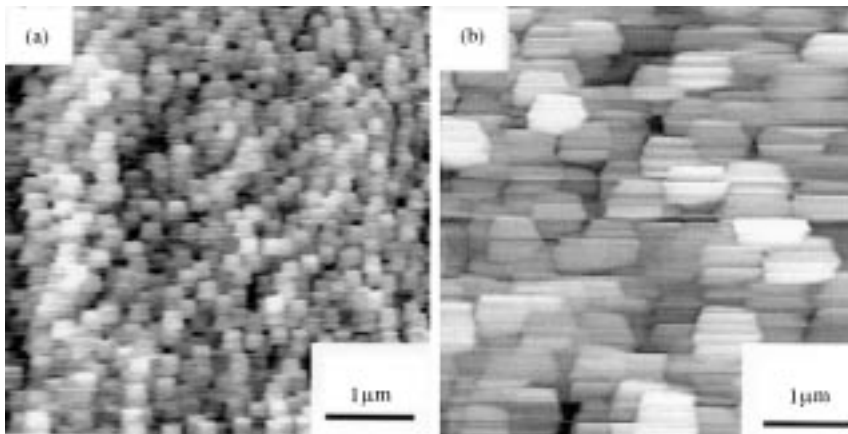


Fig. 8. AFM images obtained from the GaN buffer layer on (a) sapphire(0001) and (b)  $\text{AlO}_x/\text{Si}(111)$  substrates.

Assuming that each domain reflects the evolution of GaN nuclei formed during the buffer-layer growth, we speculate that the nucleation density of GaN on  $\text{AlO}_x/\text{Si}(111)$  is much lower than that on sapphire. Since the lateral size scale and the density of nuclei strongly influence optical and structural properties of the overlayer [11], the unique nucleation observed here is likely to affect the subsequent overlayer growth.

Finally, we believe that it is worth mentioning a clue, obtained by comparing C-AFM images, for the mechanism that possibly leads to the growth of single-crystal GaN on  $\text{AlO}_x$ . Generally it is believed that the sapphire(0001) surface on which the GaN buffer layer is grown has atomically smooth surface that contains steps and the GaN buffer layer is necessary to initiate the growth of single-crystal GaN. Thus, we expect the domain-like features seen in Fig. 8a to initiate the single-crystal GaN growth. Comparing Fig. 8a with Fig. 8b and considering the essential result that single-crystal GaN can be grown on the surface of the GaN buffer-layer on  $\text{AlO}_x$  (Fig. 8b), the domain-like features seen in Fig. 8b may play a role that initiates the single-crystal GaN growth on  $\text{AlO}_x$ , even though the lateral size of a domain-like feature seen in Fig. 8b is much larger than in Fig. 8a. Presumably, the domain-like feature seen in Fig. 8b is most likely to be tied to the domain-like feature seen on  $\text{AlO}_x$  surface (Fig. 7b). Therefore we believe that

the domain-like features seen on  $\text{AlO}_x$  surface probably play an important role to lead to single-crystal GaN growth. Similar observation of domain-like features has also been reported for GaN buffer layer grown on GaAs [12].

In summary, signal-crystal hexagonal GaN has been grown on oxidized AlAs ( $\text{AlO}_x$ ) formed on a Si(111) substrate. The surface morphology of GaN/ $\text{AlO}_x/\text{Si}(111)$  is found to be very sensitive to both the buffer-layer thickness and the  $\text{AlO}_x$  thickness. C-AFM observation indicates that the  $\text{AlO}_x$  surface appears to be composed by the domain-like features with a significant height variation. The domain-like feature evolves laterally upon a high-temperature annealing prior to the buffer-layer growth, leading to smoother surfaces. The domain-like feature seen on the  $\text{AlO}_x$  surface may be a clue for the mechanism(s) by which single crystal-GaN grows on an  $\text{AlO}_x$  layer that seems to be an amorphous/fine-grain phase.

This work has been supported by Office of Naval Research and Defense Advanced Research Projects Agency.

## References

- [1] A. Watanabe, T. Takeuchi, K. Kurosawa, H. Amano, I. Akasaki, *J. Crystal Growth* 128 (1993) 391.

- [2] T. Takeuchi, H. Amano, K. Hiramatsu, N. Sawaki, I. Akasaki, *J. Crystal Growth* 115 (1991) 634.
- [3] J.W. Yang, C.J. Sun, Q. Chen, M.Z. Anwar, M.S. Khan, S.A. Nikishin, G.A. Seryogin, A.V. Osinsky, L. Chernyak, H. Temkin, C. Hu, S. Mahajan, *Appl. Phys. Lett.* 69 (1996) 3566.
- [4] Z. Yang, F. Guarin, I.W. Tao, W.I. Wang, S.S. Iyer, *J. Vac. Sci. Technol B* 13 (1995) 789.
- [5] A.J. Steckl, J. Devrajan, C. Tran, R.A. Stall, *Appl. Phys. Lett.* 69 (1996) 2264.
- [6] J.T. Kobayashi, N.P. Kobayashi, P.D. Dapkus, *J. Electron. Mater.* 26 (1997) 1114.
- [7] N.P. Kobayashi, J.T. Kobayashi, W.-J. Choi, A.E. Bond, P.D. Dapkus, X. Zhang, D.H. Rich, presented in 1997 Summer Topical Meetings, IEEE/LEOS, Montreal, Canada, 1997.
- [8] A.R. Sugg, E.I. Chen, N. Holonyak Jr., K.C. Hsieh, J.E. Baker, N. Finnegan, *J. Appl. Phys.* 74 (1993) 3880.
- [9] B.-C. Chung, M. Gershenson, *J. Appl. Phys.* 72 (1992) 651.
- [10] M. Yoshimoto, T. Maeda, T. Ohnishi, H. Koinuma, O. Ishiyama, M. Shinohara, M. Kubo, R. Miura, A. Miyamoto, *Appl. Phys. Lett.* 67 (1995) 2615.
- [11] S. Keller, D. Kapolnek, B.P. Keller, Y. Wu, B. Heying, J.S. Speck, U.K. Mishra, S.P. Denbaars, *Jpn. J. Appl. Phys.* 35 (1996) L285.
- [12] H. Yang, O. Brandt, M. Wassermeier, J. Behrend, H.P. Schonherr, K.H. Ploog, *Appl. Phys. Lett.* 68 (1996) 244.